

# Testing improved staggered fermions with $m_s$ and $B_K$

Weonjong Lee,<sup>1,\*</sup> Tanmoy Bhattacharya,<sup>2,†</sup> George T. Fleming,<sup>3,‡</sup>  
Rajan Gupta,<sup>2,§</sup> Gregory Kilcup,<sup>4,¶</sup> and Stephen R. Sharpe<sup>5,\*\*</sup>

<sup>1</sup> School of Physics, Seoul National University, Seoul, 151-747, South Korea

<sup>2</sup> MS-B285, T-8, Los Alamos National Lab, Los Alamos, New Mexico 87545, USA

<sup>3</sup> Jefferson Lab, 12000 Jefferson Avenue, Newport News, VA 23606, USA

<sup>4</sup> Department of Physics, Ohio State University, Columbus, OH 43210, USA

<sup>5</sup> Physics Department, University of Washington, Seattle, WA 98195-1560, USA

(Dated: November 6, 2018)

We study the improvement of staggered fermions using hypercubically smeared (HYP) links. We calculate the strange quark mass and the kaon B-parameter,  $B_K$ , in quenched QCD on a  $16^3 \times 64$  lattice at  $\beta = 6.0$ . We find  $m_s(\overline{\text{MS}}, 2 \text{ GeV}) = 101.2 \pm 1.3 \pm 4 \text{ MeV}$  and  $B_K(\overline{\text{MS}}, 2 \text{ GeV}) = 0.578 \pm 0.018 \pm 0.042$ , where the first error is from statistics and fitting, and the second from using one-loop matching factors. The scale ( $1/a = 1.95 \text{ GeV}$ ) is set by  $M_\rho$ , and  $m_s$  is determined using the kaon mass. Comparing to quenched results obtained using unimproved staggered fermions and other discretizations, we argue that the size of discretization errors in  $B_K$  is substantially reduced by improvement.

PACS numbers: 11.15.Ha, 12.38.Gc, 12.38.Aw

## I. INTRODUCTION

One of the major sources of uncertainty in using precision experimental data to constrain the standard model is the lack of knowledge of the matrix elements of the effective weak Hamiltonian between hadronic states. The kaon bag parameter  $B_K$ , which parameterizes the matrix element of the  $\Delta S = 2$  operator responsible for kaon-antikaon mixing, is one such key input for the determination of the CKM mixing matrix. It is defined as the dimensionless ratio

$$B_K = \frac{\langle \bar{K}^0 | \bar{s} \gamma_\mu (1 - \gamma_5) d \bar{s} \gamma_\mu (1 - \gamma_5) d | K^0 \rangle}{\frac{8}{3} \langle \bar{K}^0 | \bar{s} \gamma_\mu \gamma_5 d | 0 \rangle \langle 0 | \bar{s} \gamma_\mu \gamma_5 d | K^0 \rangle} \quad (1)$$

Different approaches, including chiral perturbation theory, the large  $N_c$  expansion, QCD sum rules and lattice QCD, have been used to estimate  $B_K$ . The advantage of the lattice approach is that it is a first principle, non-perturbative determination. On the other hand it introduces statistical and systematic errors like those due to discretization and the matching of lattice and continuum operators. To gain control over these uncertainties, different fermion discretizations—Wilson, staggered, domain-wall (DW) and overlap—have been used in simulations.<sup>1</sup>

In this note we explore the extent to which improved staggered fermions can be used to reduce two of the most

important systematic errors, *i.e.*, those due to discretization and the matching of lattice and continuum operators. This test is carried out in the quenched approximation to get an estimate of the size of these errors by comparing with existing data. Our ultimate aim, however, is to find a method which can be used effectively on dynamical lattices likely to be produced in the near future.

Staggered fermions are an attractive choice for the calculation of weak matrix elements because they are computationally efficient—indeed, simulations with three dynamical flavors are already possible with relatively light quark masses [2]—and yet retain sufficient chiral symmetry to protect operators of physical interest from mixing with others of wrong chirality. Their disadvantage is that they retain four “tastes” of doublers for each lattice field. In the continuum limit, these four tastes become degenerate, and one can remove the additional degrees of freedom by hand. For the valence quarks this procedure is explained for the calculation of  $B_K$  in Ref. [3], while for the sea quarks one must take the fourth-root of the quark determinant. At non-zero lattice spacing, however, quark-gluon interactions violate the taste symmetry. This has three important consequences for calculations of  $B_K$ .

The first concerns taste symmetry violation and the need to take the fourth-root of the quark determinant. For non-zero lattice spacing, there is no proof that the underlying lattice action is local and lies in the same universality class as QCD. Even though we do not face this problem in quenched simulations, it is relevant when extending our calculations to dynamical simulations. Our justification for proceeding is empirical—accurate unquenched simulations using the fourth-root of the determinant find agreement between lattice and experimental results [2].

Second, large  $\mathcal{O}(a^2)$  discretization errors have been

\*Electronic address: wlee@phya.snu.ac.kr

†Electronic address: tanmoy@lanl.gov

‡Electronic address: flemingg@jlab.org

§Electronic address: rajan@lanl.gov

¶Electronic address: kilcup@physics.ohio-state.edu

\*\*Electronic address: sharpe@phys.washington.edu

<sup>1</sup> See Ref. [1] for a recent review.

TABLE I: Quark masses used in simulation and their relation to the strange quark mass.

Name	$am_q$	$m_q/m_s$
$m_1$	0.01	0.192
$m_2$	0.02	0.385
$m_3$	0.03	0.577
$m_4$	0.04	0.769

observed in the calculation of masses and matrix elements. Overcoming these requires the use of very small lattice spacings to make reliable continuum extrapolations. Lastly, many one-loop perturbative estimates of matching factors differ significantly from their tree-level value of unity, raising doubts about their accuracy [4].

The purpose of this paper is to show, using  $m_s$  and  $B_K$  as probes, that the latter two problems can be greatly alleviated by improving staggered fermions using “fat” links [5]. Based on the analysis of Ref. [6], we choose a particular type of fattening, hypercubic (HYP) smeared links [7], although we expect that other choices will work comparably well. Earlier calculations show that taste-symmetry violations in the spectrum are substantially reduced [7, 8], and one-loop corrections to matching factors for four-fermion operators which were as large as 100% are now reduced to  $\sim 10\%$  [9]. The largest improvement is in renormalization constants of left-right (penguin) four-fermion operators [9], and this can be traced back to the improvement in  $Z_m = 1/Z_S = 1/Z_P \approx 1$  with HYP smearing. This has a major impact on the extraction of  $m_s$  as we show in section III. In the case of  $B_K$  the major impact of improvement is to reduce discretization errors. This is because the one-loop corrections to matching factors in this case turn out to be small ( $\sim 10\%$ ) before (as well as after) improvement.

To test the efficacy of improvement for  $m_s$  and  $B_K$ , we compare our results to the JLQCD analyses with unimproved staggered fermions that include detailed studies of both discretization and perturbative errors [10, 11].

This paper is organized as follows. In Sec. II, we analyze the  $\rho$  meson spectrum calculated on the HYP smeared lattices and obtain the lattice scale  $1/a$ . In Sec. III, we present the extraction of strange quark mass from the pion spectrum and compare the result with that obtained using unimproved staggered fermions. In Sec. IV, we present results for  $B_K$  calculated using the HYP improved staggered fermions and compare them with those of unimproved staggered fermions and with some recent data obtained using domain wall and overlap fermion formulations. We close with some conclusions in Sec. V.

## II. $\rho$ MESON SPECTRUM

The statistical sample consists of an ensemble of 218 gauge configurations of size  $16^3 \times 64$  generated using the

Wilson plaquette action at  $\beta = 6.0$ . The lattices were first HYP smeared using the tree-level improved parameters of Ref. [6]. On these HYP smeared lattices quark propagators are calculated using 2Z wall sources on time-slices 0, 16, 32 and 48 for the bare quark masses listed in Table I. <sup>2</sup> Meson correlators are calculated at all time slices for each set of the 2Z wall sources. Throughout this work we only consider mesons composed of degenerate quarks.

The lattice scale is set using the  $\rho$  meson mass. We calculated correlators for two types of  $\rho$  mesons:  $\rho(1)$ , with spin-taste  $(\gamma_i \otimes \xi_i)$ ; and  $\rho(2)$ , with spin-taste  $(\gamma_i \gamma_4 \otimes \xi_i \xi_4)$ . The correlators are fit to the standard form [13]:

$$C(t) = Z_1 \{ \exp[-m_1 t] + \exp[-m_1(L-t)] \} + Z_2 (-1)^t \{ \exp[-m_2 t] + \exp[-m_2(L-t)] \} \quad (2)$$

where  $m_1$  is the mass of the  $\rho$  meson, while  $m_2$  is the mass of its opposite parity partner, whose contribution has an alternating sign in the time direction. The partner for  $\rho(1)$  is the  $b_1$  meson, with spin-taste  $(\gamma_j \gamma_k \otimes \xi_j \xi_k)$ , while that for the  $\rho(2)$  is the  $a_1$  with spin-taste  $(\gamma_i \gamma_5 \otimes \xi_i \xi_5)$ .

We obtain good fits to both  $\rho$  correlators except for the  $\rho(1)$  at the lightest quark mass. The resulting masses, as well as those of the parity partner  $a_1$ , are given in Table II. Since we want to be able to use all four quark masses to carry out the chiral extrapolation, we opt to consider only the  $\rho(2)$  results to determine the lattice scale. We do not, however, expect that the resulting scale would change significantly were we to use  $\rho(1)$  masses, because the  $\rho(1)$  and  $\rho(2)$  masses agree within errors for the three heavier quark masses. To illustrate the quality of the fits we show the effective mass plots for  $\rho(2)$  as a function of time in Figs. 1-4. The effective mass at time  $t = T$  is defined to be the value of  $m_1$  obtained by solving Eq. (2) using the correlation function on time slices  $T$  to  $T + 3$ . All errors are determined using single elimination jackknife, with the underlying fits (both in  $t$  and  $m$ ) using uncorrelated errors, because the correlation matrix is determined with insufficient accuracy.

The result of a quadratic fit to  $M_{\rho(2)}$  versus quark mass, shown in Fig. 5, is

$$aM_\rho = 0.399(10) + 2.60(59)(am_q) - 9.3(8.7)(am_q)^2. \quad (3)$$

From this we estimate the lattice scale  $1/a$  quoted in Table II by setting the chirally extrapolated value  $0.399(10) = aM_\rho^{physical}$ . The change in the resulting scale from extrapolating to the physical light quark masses  $(a(m_u + m_d))/2 \sim 0.0015$  rather than the chiral limit is smaller than our statistical errors and we do not include it. We also do not include the  $m_q^{1/2}$  and  $m_q^{3/2}$  terms from pion loops [14] in our chiral fit, as they are expected to have small coefficients, and we have too few mass points to reliably include them.

<sup>2</sup> The details on the 2Z wall source are given in Ref. [12].

TABLE II: Masses of  $\rho$  and  $a_1$  mesons, and resulting scales.

$m_q$	$aM_\rho(\gamma_i \otimes \xi_i)$	$aM_\rho(\gamma_i\gamma_4 \otimes \xi_i\xi_4)$	$aM_{a_1}(\gamma_i\gamma_5 \otimes \xi_i\xi_5)$
$m_1$	—	0.4244(63)	0.5897(345)
$m_2$	0.4444(32)	0.4466(40)	0.6350(218)
$m_3$	0.4676(32)	0.4692(43)	0.6387(347)
$m_4$	0.4865(25)	0.4879(32)	0.6657(250)
$1/a$	—	1945(50) MeV	2112(131) MeV

A potential problem with our estimate of the scale is our use of a relatively small volume ( $L \approx 1.6$  fm). Although we expect this is large enough to study kaon properties (since  $m_K L \approx 5$  is larger than the range 3–4 where significant effects usually set in), we are relying in our scale determination on results from all four quark masses. At the lightest quark mass  $M_\pi L = 2.7$ , and volume errors may be significant. Evidence that this is the case comes from Ref. [11], who have results for  $M_\rho$  for three different volumes at  $\beta = 6$ . The finite volume effects can be seen from the resulting estimates of the scale:  $1/a = 1.87(6)$ ,  $1.88(4)$  and  $2.01(2)$  GeV, for  $18^3$ ,  $24^3$  and  $32^3$  lattices, respectively. Thus we may have underestimated the scale by  $\approx 7\%$ . It turns out, however, that this uncertainty is smaller than the range of scales resulting from the use of different physical quantities, and so can be subsumed into the quenching error discussed below.

Data for the  $a_1$  meson has much larger errors and we use a simple linear fit. The result, shown in Fig. 6, gives

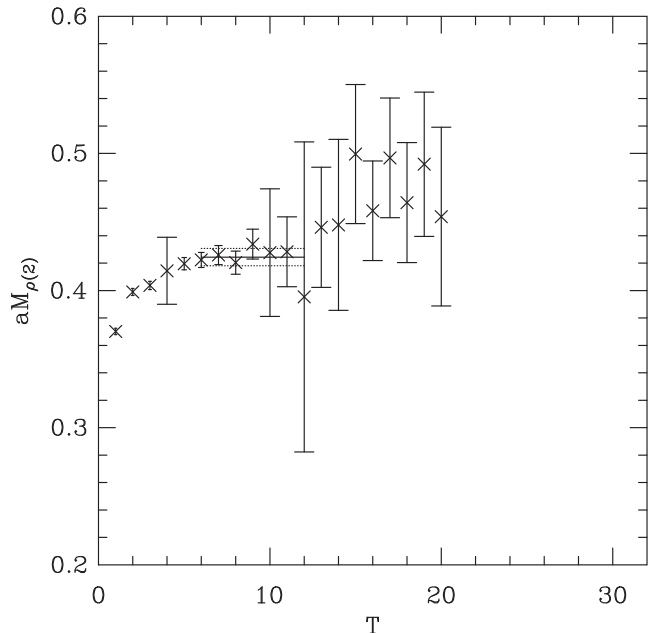
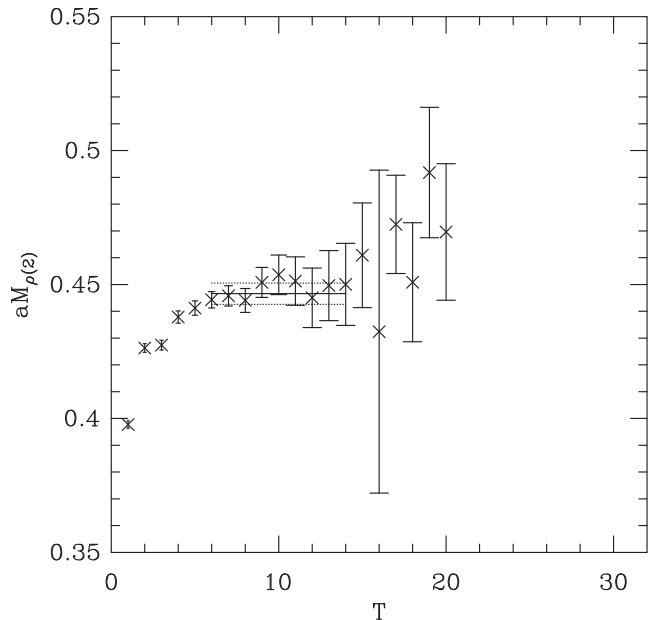
$$aM_{a_1} = 0.58(4) + 2.1(1.0)(am_q) \quad (4)$$

Again, the chirally extrapolated value is used to determine the estimate of  $1/a$  given in Table II.

One of the well-known uncertainties introduced by quenching is that different physical quantities lead to different values of the lattice spacing. Since we are interested here in comparing with other quenched results for  $m_s$  and  $B_K$ , we follow most previous calculations and determine our central value for the scale,  $1/a = 1.95$  GeV, using  $\rho$  masses. This lies within the range of values quoted above from the JLQCD  $B_K$  calculation, and is close to the value,  $1/a = 1.855(38)$  GeV, they use when estimating  $m_s$  [10]. Nevertheless, to understand the impact of the scale uncertainty, and, as noted above, to include possible finite volume errors, we also analyze subsequent data using  $1/a = 2.1$  GeV. This value is consistent with our estimate from  $a_1$  as well as the result obtained using the Sommer parameter  $r_0$  [15] ( $1/a = 2.12$  GeV). The latter is derived from the static  $q\bar{q}$  potential and thus is independent of the fermion action.

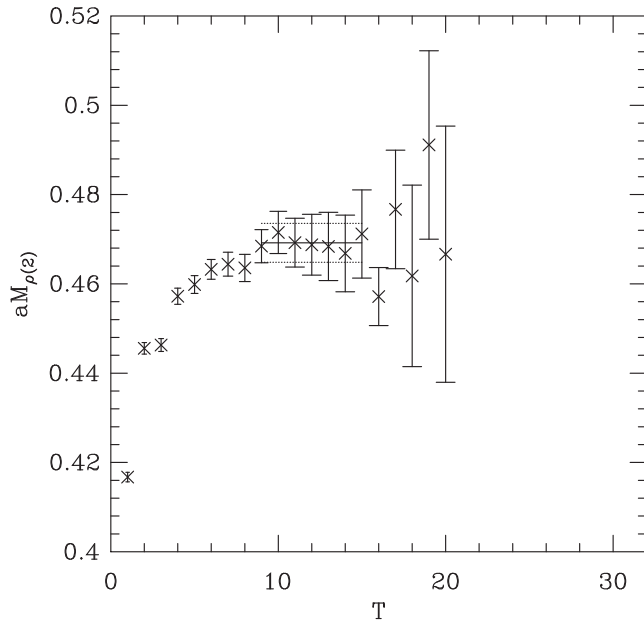
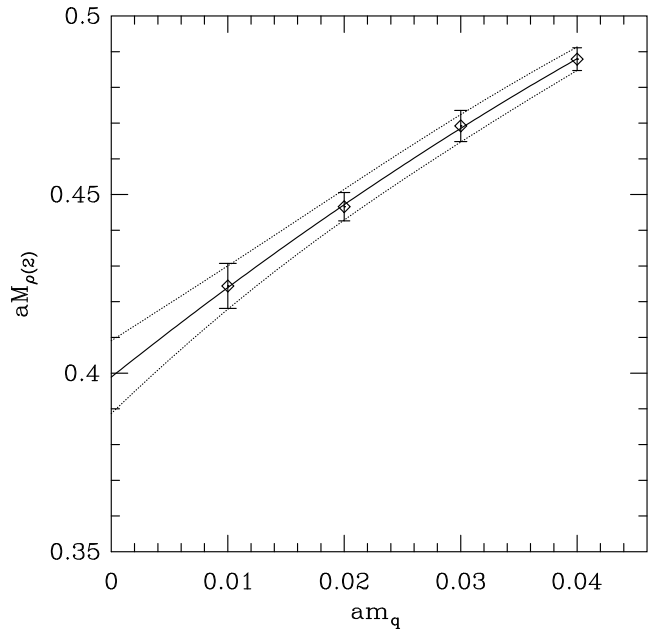
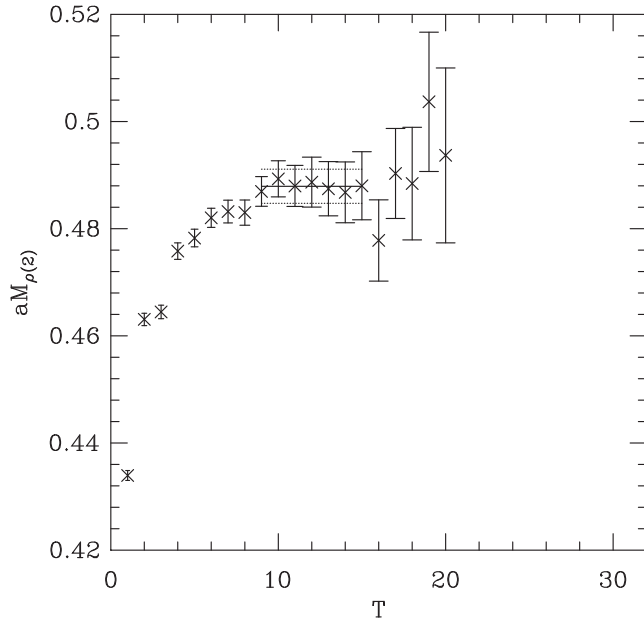
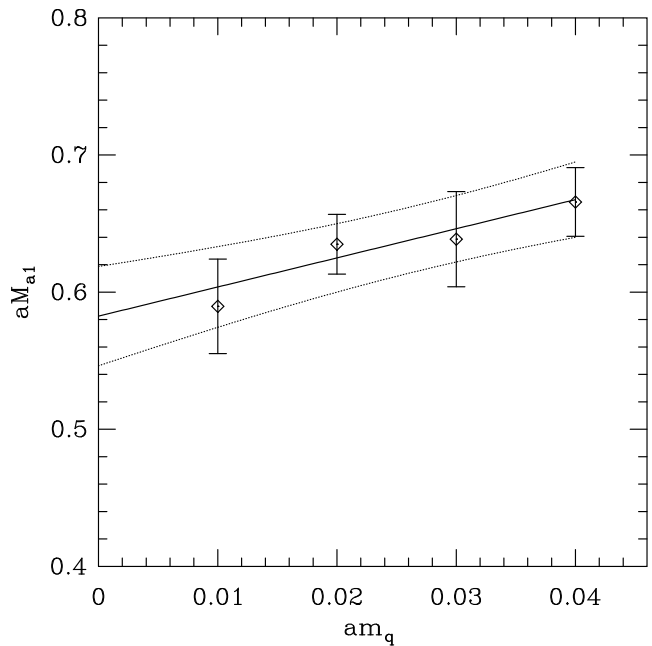
### III. STRANGE QUARK MASS

Our results for the masses of the lattice pseudo-Goldstone pion (spin-taste  $\gamma_5 \otimes \xi_5$ ) are presented in Table III. The results with different sources and sinks are

FIG. 1: Effective mass plot of  $aM_\rho$  at quark mass 0.01.FIG. 2: Effective mass plot of  $aM_\rho$  at quark mass 0.02.

consistent, and we use the weighted average of the four results in the subsequent analysis.

The strange quark mass  $m_s$  is determined by requiring a fictitious  $\bar{s}s$  pseudoscalar mass to match the physical value of  $(2M_K^2 - M_\pi^2)$  which corresponds to  $(aM_{PS})^2 = 0.1234$  with  $1/a = 1.95$  GeV. A linear fit for  $(aM_{PS})^2$  versus  $am_q$  works well, as shown in Fig. 7. This fit gives  $am_s = 0.0520(7)$ , and thus  $m_s = 102(1.3)$  MeV. Repeating the analysis with  $1/a = 2.1$  GeV leads instead to  $110(1.5)$  MeV. We stress that these results are not

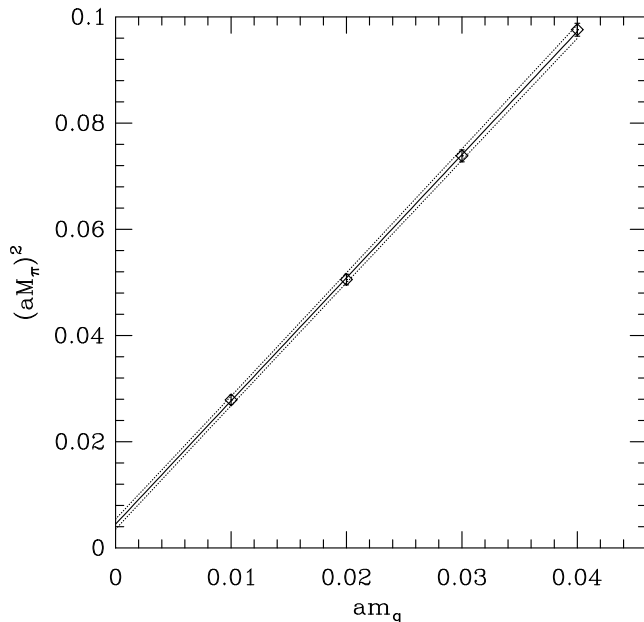
FIG. 3: Effective mass plot of  $aM_\rho$  at quark mass 0.03.FIG. 5:  $aM_\rho$  vs. quark mass.FIG. 4: Effective mass plot of  $aM_\rho$  at quark mass 0.04.FIG. 6:  $aM_{a1}$  vs. quark mass.TABLE III: Pion masses using axial and pseudoscalar operators from Left ( $t = 10$ ) and Right ( $t = 36$ ) wall sources.

$m_q$	$aM_\pi(A_4, L)$	$aM_\pi(A_4, R)$	$aM_\pi(P, L)$	$aM_\pi(P, R)$
$m_1$	0.1697(29)	0.1682(30)	0.1658(50)	0.1644(56)
$m_2$	0.2266(27)	0.2255(28)	0.2248(40)	0.2224(42)
$m_3$	0.2732(27)	0.2725(26)	0.2716(35)	0.2695(34)
$m_4$	0.3136(27)	0.3134(24)	0.3120(32)	0.3106(30)

very sensitive to the chiral fit form used. For example, a fit that includes a quenched chiral logarithm [16, 17]

and is forced to pass through the origin reduces  $m_s$  by 2.1(6) MeV. Such consistency is not surprising since  $am_s = 0.052$  is larger than the simulated points, whereas quenched chiral logarithms are important only at masses smaller than  $am_q = 0.01$ .

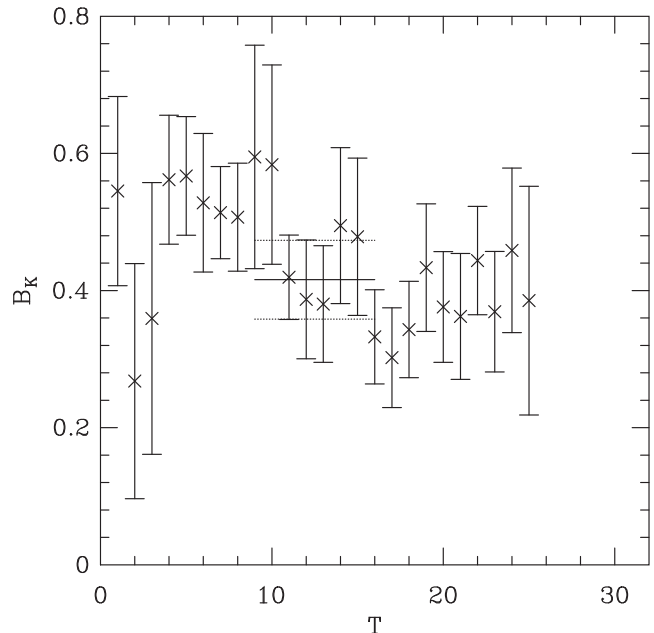
As discussed in the previous section, we expect that finite volume effects should be small in our determination of  $m_s$ , because our heaviest two quark masses dominate the determination, and these have relatively large values of  $M_\pi L$ , 4.3 and 5.0 respectively. According to the

FIG. 7:  $(aM_\pi)^2$  vs. quark mass.

quenched chiral perturbation theory analysis of Ref. [17], one would expect  $M_\pi^2$  to be larger than its infinite volume value by 1-2% in this quark mass range. This would lead to our finite volume result for  $m_s$  being 1-2% smaller than the infinite volume value. This estimate assumes the quenched hairpin parameter to be  $\delta \approx 0.2$ ; using more recent values of  $\delta \approx 0.1$  reduces the effect proportionally. That the finite size effects are no larger than this size is supported by the numerical analysis of finite volume effects given in Ref. [18].

Finite volume errors also enter into our result for  $m_s$  through their effect on the scale, as discussed in the previous section. We choose, however, to quote a value for  $m_s$  for a definite choice of scale, so as to allow more straightforward comparison with other results. In particular, using the one-loop matching factor from Ref. [6], and the scale  $1/a = 1.95$  GeV, we find the renormalized mass  $m_s(\overline{\text{MS}}, 2 \text{ GeV}) = 101.2 \pm 1.3 \pm 4$  MeV. Here the first error is statistical, while the second is from the systematic effects that we control aside from the scale uncertainty. It is dominated by the uncertainty in  $Z_m$ , which we estimate as 4% by assuming a two-loop term of size  $\pm 1 \times (\alpha_s)^2$ . It also contains the uncertainty from the form of chiral fit used, and from the finite volume errors in  $M_\pi^2$  discussed in the previous paragraph. Note that we take the central value from the fit form without quenched chiral logarithms so as to better compare to the results of Ref. [10].

This result for  $m_s$  allows us to study the efficacy of HYP improved staggered fermions. The state-of-the-art quenched estimate for unimproved staggered quarks (obtained using the same definition of  $m_s$ , and  $M_{\rho(1)}$  for setting the scale) is  $m_s(\overline{\text{MS}}, 2 \text{ GeV}) = 106.0 \pm 7.1$  MeV, after extrapolation to the continuum limit [10]. Our first

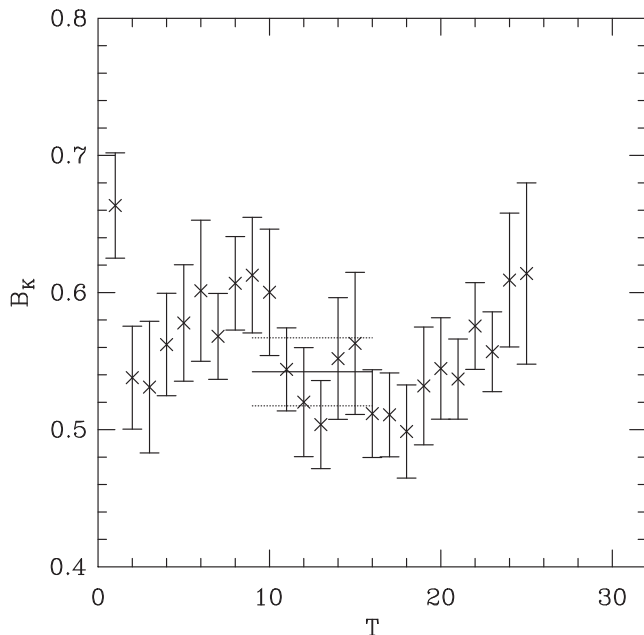
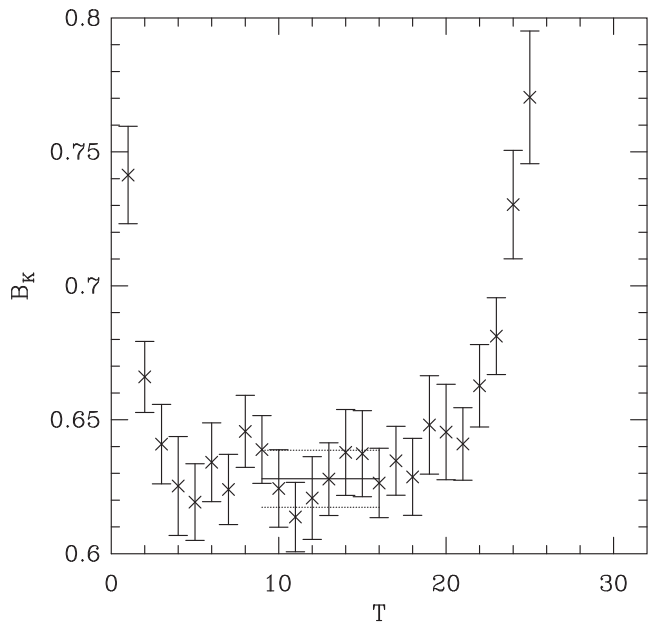
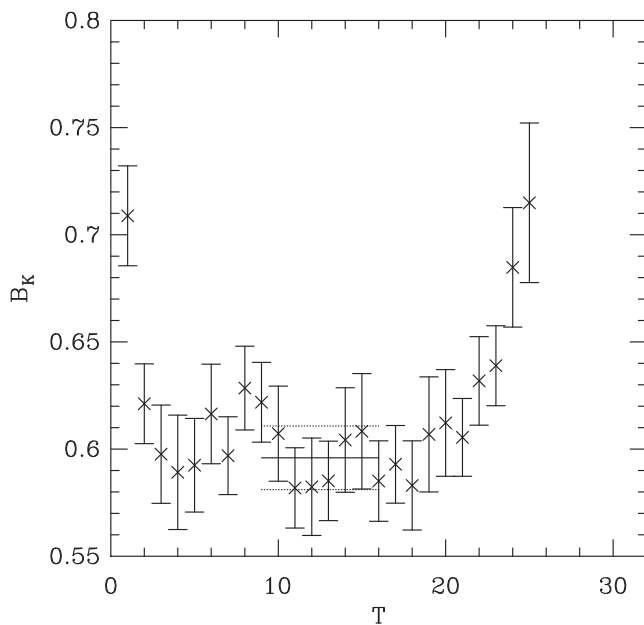
FIG. 8:  $B_K$  at quark mass 0.01.

observation is that our result at  $\beta = 6.0$  agrees with this continuum value, consistent with our expectation that  $a^2$  errors should not be large. In this respect, we note that it was necessary to go down to lattice spacing  $a = 0.06$  fm with unimproved staggered fermions in order to obtain the continuum estimate [10].

It is also useful to compare with the results from Ref. [10] obtained at our coupling,  $\beta = 6$ . Their bare quark mass,  $am_s = 0.0244$  or  $m_s = 45$  MeV, is much smaller than ours. Using non-perturbative renormalization they find  $m_s(\overline{\text{MS}}, 2 \text{ GeV}) = 114$  MeV. The very large matching factor,  $Z_m \approx 2.5$ , shows the need for non-perturbative renormalization with unimproved staggered fermions. Indeed, using one-loop matching they find the significantly smaller value  $m_s(\overline{\text{MS}}, 2 \text{ GeV}) = 84$  MeV. By contrast, our matching factor is very close to unity, illustrating one of the advantages of HYP smeared staggered fermions.

Quantifying improvement in discretization errors is more difficult. The unimproved (but non-perturbatively renormalized) result drops by 8 MeV between  $\beta = 6$  and the continuum, whereas our result is 5 MeV lower than the continuum value. Since these differences are comparable to the errors, the only definite conclusion we can draw is that the discretization errors appear to not be worsened by improvement.<sup>3</sup>

<sup>3</sup> This conclusion is bolstered by the fact that Ref. [10] uses a smaller scale than us (1.85 rather than 1.95 GeV). Had they used the larger scale, their final result at  $\beta = 6$  would have differed more from the continuum value.

FIG. 9:  $B_K$  at quark mass 0.02.FIG. 11:  $B_K$  at quark mass 0.04.FIG. 10:  $B_K$  at quark mass 0.03.

#### IV. $B_K$

The ratio of correlators corresponding to Eq. 1 is measured on the interval  $1 \leq t \leq 25$  between two random  $U(1)$  sources [19] placed at  $t = 0$  and 26. We find that the individual pseudoscalar meson correlators exhibit contamination from excited states up to  $\approx 9$  time slices from the sources. For this reason we choose to make constant fits to the central part of the plateau on time slices  $9 \leq t \leq 16$  even though the estimate is sta-

TABLE IV: Results for bare  $B_K$ ,  $B_K(\overline{\text{MS}}, \mu = 1/a, L)$  and estimate of finite volume shift:  $\delta B_K(L) = B_K(L = \infty) - B_K(L)$ . Errors are statistical.

$m_q$	bare $B_K$	$B_K(1/a, L)$	$\delta B_K(1/a, L)$
$m_1$	0.514(61)	0.416(57)	+0.0094(38)
$m_2$	0.614(26)	0.542(25)	+0.0013(5)
$m_3$	0.658(16)	0.596(15)	-0.0003(1)
$m_4$	0.686(11)	0.628(11)	-0.0006(2)

ble over the range  $4 \leq t \leq 20$ . These fits are shown in Figs. 8-11. In the first column of Table IV we give the resulting bare values for  $B_K$ , *i.e.* with all renormalization constants set to unity, for each of the quark masses. In the second column we give the results after renormalization to  $\overline{\text{MS}}$ , NDR scheme at scale  $\mu = 1/a$ .

To quote results in the  $\overline{\text{MS}}$  scheme we use the one loop renormalization factors of Ref. [9], with the matching scale chosen to be  $q^* = 1/a$ . The coupling  $\alpha_s(q^* = 1/a) = 0.192$  is calculated from the plaquette expectation value ( $P = 0.59367$ ) using the method of Ref. [20]. At the physical kaon mass, which corresponds to  $am_q = 0.026$ , the one-loop corrections lead to a  $\sim 10\%$  change in  $B_K$ . This is very similar to the corresponding shift with unimproved staggered fermions.

To extract  $B_K$  at the physical kaon mass we fit the data to the form predicted by quenched chiral perturbation

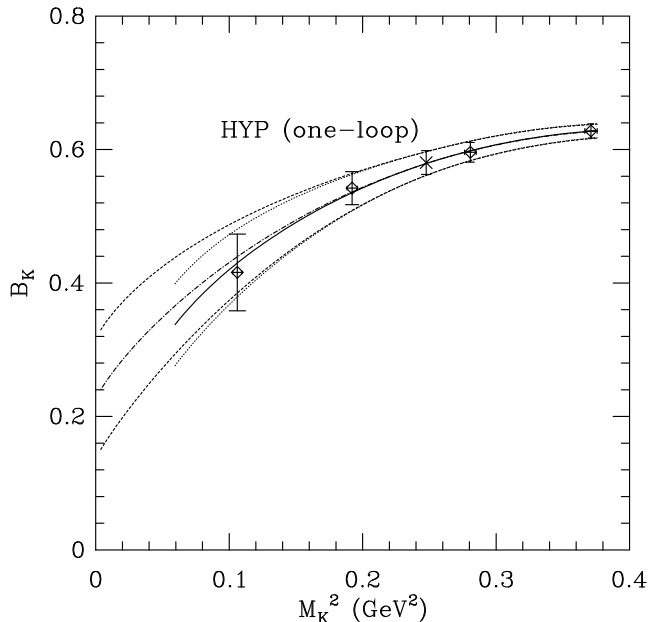


FIG. 12: Results for  $B_K(NDR, \mu = 1/a)$  (diamonds), fit to the expected chiral form at finite volume (solid line, errors small dashes). The dot-dashed line (errors long dashes) is the corresponding infinite volume result. The cross is the infinite volume result at the physical kaon mass.

theory including finite volume corrections [17]

$$\begin{aligned}
 B_K = & b_0 \left\{ 1 - 6.0 \frac{M_K^2}{(4\pi f)^2} \log \left[ \frac{M_K^2}{(4\pi f)^2} \right] \right. \\
 & \left. + \frac{2}{f^2} [-2g_1(M_K^2, 0, L) + M_K^2 g_2(M_K^2, 0, L)] \right\} \\
 & + b_1 M_K^2 + b_2 M_K^4 \quad (5)
 \end{aligned}$$

where  $f$  is the decay constant, which we fix to 132 MeV. The finite volume dependence enters through the functions  $g_i$ , defined in Ref. [21]. This dependence of  $B_K(NDR, \mu = 1/a)$  on the quark mass is shown by the solid line in Fig. 12 with parameter values  $b_0 = 0.23(9)$ ,  $b_1 = 0.5(1.1)/\text{GeV}^2$  and  $b_2 = -1.2(1.3)/\text{GeV}^4$ . Since the prediction for the finite volume corrections becomes unreliable once  $M_K L$  becomes small, we do not display the fit function below  $M_K L = 2$ .

Our results are consistent with the curvature predicted by the chiral logarithm in Eq. (5). Indeed, we can set  $b_2 = 0$  and obtain a good fit [with  $b_0 = 0.283(29)$  and  $b_1 = -0.30(19) \text{ GeV}^{-2}$ ], showing that the curvature can be accounted for by the logarithm alone. Another consistency check is that  $b_1$  and  $b_2$  agree with the expectations of naive dimensional analysis, namely  $|b_1| \approx |b_2| \approx 1$  in units of the scale,  $\sim 1 \text{ GeV}$ , of chiral perturbation theory. Taken as a whole, previous work is inconclusive concerning the presence of the chiral logarithm with predicted coefficient, largely due to the relatively high quark masses used ( $m > m_s/2$ ). It is only by extending

the range to  $m_s/5$  that we find evidence, albeit not conclusive, for the onset of the expected chiral logarithm at small quark masses.

It is important to obtain a good fit to the chiral behavior in order to reliably extract estimates of finite volume corrections. The smallest value of  $M_K L$  is 2.64, so one expects such corrections to be large [22]. For  $B_K$ , however, the cancellation between  $g_1$  and  $g_2$  terms suppresses these corrections. Based on our chiral fit, the third column in Table IV gives estimates for this finite volume shift. Note that the correction is non-monotonic in  $M_K$ , due to the cancellation noted above. The infinite volume prediction is shown in Fig. 12. From this we conclude that for physical  $M_K$  the finite volume shift in  $B_K$  is much smaller than quoted errors even on our small lattices. This conclusion is supported by the absence of finite volume errors in the JLQCD results at  $\beta = 6$  using unimproved staggered fermions [11].

Our final results are obtained by evolving from  $1/a$  to  $\mu = 2 \text{ GeV}$  using two-loop renormalization group running for  $N_f = 0$  [23]. We find

$$B_K(NDR, 2 \text{ GeV}) = 0.578 \pm 0.018 \pm 0.042, \quad (6)$$

$$B_K^{RGI} = 0.806 \pm 0.025 \pm 0.058, \quad (7)$$

$$b_0^{RGI} = 0.314 \pm 0.124 \pm 0.176. \quad (8)$$

where  $B_K^{RGI}$  is the renormalization group invariant  $B$ -parameter [23], with  $b_0^{RGI}$  its value in the chiral limit. The first error combines that from statistics and those due to the chiral interpolation (or extrapolation for  $b_0$ ). The second is our estimate of the uncertainty from using one-loop matching factors explained below. Aside from the errors due to quenching and the use of degenerate quarks, which we do not address here, other systematics lead to changes smaller than the perturbative error. For example, using the scale from  $r_0$  reduces  $B_K(NDR, 2 \text{ GeV})$  and  $b_0^{RGI}$  by 0.025 and 0.007, respectively, while setting  $b_2 = 0$  in the chiral fit increases them by 0.011 and 0.079. If we use  $f = f_K = 159.8 \text{ MeV}$  instead of  $f = 132 \text{ MeV}$  in Eq. 5 and fit the data,  $B_K$  changes by less than 0.01%, while  $b_0$  increases by 5%.

The error associated with unknown  $\alpha^2$  corrections is estimated as follows. We can write  $B_K = B_A + B_V$ , where  $V$  and  $A$  refer to vector-vector and axial-axial parts of the operator in Eq. (1).  $B_{A,V}$  can each be decomposed into one and two color-trace parts [3]. Each of these four components of  $B_K$  is proportional to  $\log(M_K^2)$  and thus diverges in the chiral limit, although their sum does not. Using one-loop matching there is an incomplete cancellation, and the resulting  $B_K$  should diverge in the chiral limit, although this feature is expected to manifest itself at much smaller quark masses than studied here. Indeed, the bare values for  $B_{V,A}$  do indicate a divergent behavior. Because of the residual divergence, we cannot simply estimate the error, in particular in  $b_0$ , by multiplying by an overall relative correction of  $\pm \alpha(q^*)^2$  (as we did for  $m_s$ ). Instead, we recalculate  $B_K$  after adding  $\pm \alpha(q^*)^2$  to the matching factors for each of the four components of

TABLE V:  $B_K(\text{NDR}, 2 \text{ GeV})$  at  $\beta = 6$  for gauge invariant (GI) and non-invariant (NGI) operators, before and after removing the fitted  $a^2$  and  $\alpha^2$  terms. Data from Ref. [11].

Type	Uncorrected	$a^2$ removed	$\alpha^2$ removed
GI	0.6790(16)	0.55(7)	0.76(7)
NGI	0.7128(14)	0.61(7)	0.73(7)

$B_K$  in turn, and take the largest variation as the error. The resulting uncertainty, quoted above, is larger than the statistical error and, as expected, grows rapidly in the chiral limit.

Even though we need more high precision data at lighter quark masses to pin down the chiral extrapolation, it is nevertheless interesting that our estimate  $b_0^{RGI} = 0.314 \pm 0.124 \pm 0.176$  is in good agreement with recent estimates 0.29(15) [24] and 0.36(15) [25] obtained using  $1/N_c$  expansion.

We now compare our estimate with the state-of-the-art results obtained by the JLQCD collaboration [11] using unimproved staggered fermions and argue that HYP smearing reduces discretization errors. The JLQCD result in the continuum limit is  $B_K(\text{NDR}, 2 \text{ GeV}) = 0.628 \pm 0.042$ . Our first observation is that our result at  $\beta = 6$  is consistent with this continuum result. On the one hand, this indicates that the  $a^2$  errors with HYP fermions are not large, as for  $m_s$ . On the other hand, the value of  $B_K$  at  $\beta = 6$  with unimproved staggered fermions [0.679(2)] is also consistent with the continuum result, giving no evidence of improvement.

We can go further, however, using the details of the continuum extrapolation provided by Ref. [11]. Their fit included both  $a^2$  and  $\alpha_s^2$  terms. Using their fit parameters we can determine two additional estimates of  $B_K$  at  $\beta = 6.0$ : removing only the  $O(a^2)$  term (and not the  $O(a^2)$  discretization correction) and vice-versa. The original results and those corrected for either the discretization or perturbative errors alone are given in Table V. The point we wish to make is that in the case of gauge invariant operators (which are those we use) the JLQCD fits imply that, at  $\beta = 6$ , the total result 0.68 contains an  $O(a^2)$  contribution of  $\sim 0.13$  and an  $O(\alpha^2)$  contribution of  $\sim -0.08$ . (Corrections for non gauge-invariant operators, which are not the operators of choice, are somewhat smaller but show the same pattern.) Thus, in a formulation where only discretization errors were eliminated or substantially reduced one should expect a final result closer to 0.55 at  $a \approx 0.1$  fermi. Our estimate with HYP smearing,  $B_K(\text{NDR}, 2 \text{ GeV}) = 0.58(4)$ , is indeed consistent with this and significantly different from the unimproved JLQCD result 0.679(2). This suggests that discretization errors have been reduced by using HYP smeared fermions.

This conclusion is supported by the fact that all calculations with domain wall or overlap fermions, which are also expected to have small discretization errors and small perturbative corrections, find values at  $\beta = 6$  consistent with ours: 0.575(6) (Ref. [26]), 0.532(11) (Ref. [27]), 0.563(31) (mean of data at  $\beta = 5.9$  and 6.1 in Ref. [28]), and 0.63(6) (Ref. [29]). Here, only statistical errors have been quoted.

Finally, we consider the results in Table V with “ $\alpha^2$  removed”. These correspond approximately to using non-perturbative matching factors, and should thus expose the “true”  $a^2$  errors in the unimproved results. Unfortunately, the large errors preclude definitive conclusions. Nevertheless, the fact that our result 0.58(4) differs from the “ $\alpha^2$  removed” unimproved result of 0.76(6) by about  $2\sigma$ , while lying closer to the continuum result 0.62(4), is consistent with our conclusion that discretization errors are reduced by using smeared links.

## V. CONCLUSION

We conclude that improved staggered fermions are a viable and promising option for calculations of  $m_s$  and  $B_K$  in full QCD simulations. The difficulties observed with unimproved staggered fermions (ill behaved perturbation theory for  $Z_m$  in the case of  $m_s$  and discretization errors in  $B_K$ ) are greatly reduced. Our study suggests that reliable calculations should be possible on the ensembles of lattices being generated with dynamical improved staggered fermions without requiring very small lattice spacings. There are two caveats, however. To reduce the uncertainty due to the two-loop term in the renormalization constants below our estimates of 4% in  $m_s$  and 7% in  $B_K$  will require a demanding two-loop or non-perturbative calculation of matching factors and the calculation of a larger set of lattice matrix elements. Second, in the case of  $B_K$ , the estimate in the chiral limit is very sensitive to errors in the matching factors, as well as to the chiral extrapolation.

## VI. ACKNOWLEDGEMENT

This calculation has been done on Columbia QCDSF supercomputer. We thank N. Christ, C. Jung, C. Kim, G. Liu, R. Mawhinney and L. Wu for their support on this staggered  $\epsilon'/\epsilon$  project. This work is supported in part by BK21, by Interdisciplinary Research Grant of Seoul National University and by KOSEF contract R01-2003-000-10229-0, the US-DOE grant KA-04-01010-E161 and contract DE-FG02-96ER40956. We gratefully acknowledge discussions with A. Soni.

[1] D. Becirevic, Nucl. Phys. B (Proc. Suppl.) **129 & 130**, 34 (2004).

[2] C. T. H. Davies *et al.*, Phys. Rev. Lett. **92**, 022001 (2004).



- [3] G. Kilcup, R. Gupta and S. R. Sharpe, Phys. Rev. D **57**, 1654 (1998).
- [4] M. Golterman, Nucl. Phys. B Proc. Suppl. **73**, 906 (1999).
- [5] J. F. Lagae and D. K. Sinclair, Phys. Rev. D **59**, 014511 (1999); G. P. Lepage, *ibid.* 074502.
- [6] W. Lee and S. Sharpe, Phys. Rev. D **66**, 114501 (2002).
- [7] A. Hasenfratz and F. Knechtli, Phys. Rev. D **64**, 034504 (2001).
- [8] K. Orginos and D. Toussaint [MILC collaboration], Phys. Rev. D **59**, 014501 (1999).
- [9] W. Lee and S. Sharpe, Phys. Rev. D **68**, 054510 (2003).
- [10] S. Aoki, *et al.*, Phys. Rev. Lett. **82**, 4392 (1999).
- [11] S. Aoki, *et al.*, Phys. Rev. Lett. **80**, 5271 (1998).
- [12] C. Sui, PhD. Thesis, Columbia University (2000).
- [13] M.F. Golterman, Nucl. Phys. B **273**, 663 (1986).
- [14] M. Booth, G. Chiladze and A. F. Falk, Phys. Rev. D **55**, 3092 (1997).
- [15] R. Sommer, Nucl. Phys. **B411**, 839 (1994).
- [16] C. W. Bernard and M. F. L. Golterman, Phys. Rev. D **46**, 853 (1992).
- [17] S. Sharpe, Phys. Rev. D **46**, 3146 (1992).
- [18] S. Aoki, *et al.*, Phys. Rev. D **50**, 486 (1994).
- [19] D. Pekurovsky and G. Kilcup, Phys. Rev. D **64**, 074502 (2001).
- [20] C.T.H. Davies, *et al.*, Phys. Rev. D **56**, 2755 (1997).
- [21] J. Gasser and H. Leutwyler, Phys. Lett. B **184**, 83 (1987); **188**, 477 (1987).
- [22] D. Becirevic and G. Villadoro, Phys. Rev. D **69**, 054010 (2004).
- [23] J. Buras, M. Jamin, and P. Weisz, Nucl. Phys. B **347**, 491 (1990).
- [24] J. Prades, J. Bijnens and E. Gamiz arXiv:hep-ph/0501177
- [25] O. Cata and S. Peris, JHEP **0303**, 060 (2003).
- [26] A. Ali Khan, *et al.*, Phys. Rev. D **64**, 114506 (2001).
- [27] T. Blum, *et al.* [RBC Collaboration], Phys. Rev. D **68**, 114506 (2003).
- [28] Thomas DeGrand, Phys. Rev. D **69**, 014504 (2004).
- [29] Nicolas Garron, *et al.*, Phys. Rev. Lett. **92**, 042001 (2004).